Downloaded from orbit.dtu.dk on: May 05, 2023

DTU Library

Three-Phase Modulated Pole Machine Topologies Utilizing Mutual Flux Paths

Washington, Jamie G. ; Atkinson, Glynn J. ; Baker, Nick J. ; Jack, Alan G. ; Mecrow, Barrie C. ; Jensen, Bogi Bech; Pennander, Lars-Olov ; Nord, Göran L. ; Sjöberg, Lars

Published in:
IEEE Transactions on Energy Conversion

Link to article, DOI:
10.1109/TEC.2012.2184115

Publication date:
2012

Link back to DTU Orbit

Citation (APA):
Washington, J. G., Atkinson, G. J., Baker, N. J., Jack, A. G., Mecrow, B. C., Jensen, B. B., Pennander, L-O., Nord, G. L., & Sjöberg, L. (2012). Three-Phase Modulated Pole Machine Topologies Utilizing Mutual Flux Paths. *IEEE Transactions on Energy Conversion*, *27*(2), 507-515. https://doi.org/10.1109/TEC.2012.2184115

General rights
Copyright and moral rights for the publications made accessible in the public portal are retained by the authors and/or other copyright owners and it is a condition of accessing publications that users recognise and abide by the legal requirements associated with these rights.

- Users may download and print one copy of any publication from the public portal for the purpose of private study or research.
- You may not further distribute the material or use it for any profit-making activity or commercial gain
- You may freely distribute the URL identifying the publication in the public portal

If you believe that this document breaches copyright please contact us providing details, and we will remove access to the work immediately and investigate your claim.

Three-Phase Modulated Pole Machine Topologies Utilizing Mutual Flux Paths

Jamie G. Washington, Glynn J. Atkinson, Nick J. Baker, Alan G. Jack, Barrie C. Mecrow, Bogi B. Jensen, Lars-Olov Pennander, Göran L. Nord, and Lars Sjöberg

***Abstract*—This paper discusses three-phase topologies for modulated pole machines (MPMs). The authors introduce a new three-phase topology, which takes advantage of mutual flux paths; this is analyzed using 3-D finite-element methods and compared to a three-phase topology using three single-phase units stacked axially. The results show that the new "combined-phase MPM" exhibits a greater torque density, while offering a reduction in the number of components. The results obtained from two prototypes are also presented to verify the concept; the results show that the "combined-phase" machine could provide both performance and constructional benefits over prior MPM topologies.**

***Index Terms*—AC machine, modulated pole, mutual flux path, permanent magnet machine, phase isolation, three phase, transverse flux, torque dense.**

I. Introduction

MODULATED pole machines (MPMs) have existed for more than 100 years, with a design first proposed by W. M. Morday [1]. The MPM topology has been developed over the years; they are often found in the form of claw pole [2], [3] and transverse flux machines (TFMs) [4].

MPMs are known for their high torque densities, often up to 5 times that of conventional machines [5]. This is due to the decoupled nature of the electric and magnetic circuits of the machine. In conventional machines, a doubling in pole number will lead to a reduction in the armature magnetomotive force (MMF) per pole by the same proportion due to a reduced slot area. Hence, there is no increase in torque as a result.

In MPMs, the MMF is seen across all of the poles; an increase in pole number does not decrease the available slot area; hence, for an increase in pole number, there is a corresponding increase in the electrical loading and therefore an increase in torque [6].

MPMs are particularly suited to low-speed applications where a high torque is required [7]; they exist in linear [8]–[11] and rotary [12] forms, and commonly have two [13] or three phases [12]. Target applications have included propulsion systems for ships [14], buses [15], cars [16], as well as renewable energy systems such as generators in direct drive wind turbines [17] and wave energy generation [18], [19]. Their speed is limited by the frequency of available electrical converters due to the high electrical frequency required as a consequence of the high pole number. These machines can also exhibit a high reactance, resulting in a low power factor [20], thus, requiring a converter with a higher voltampere rating.

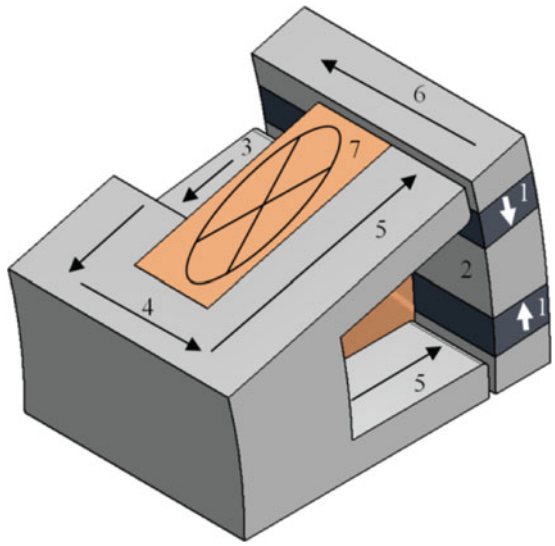

Fig. 1. Two pole section of a single phase.

The term "MPM" captures all machine types where a two-pole armature field is guided or "modulated" into many poles by a toothed iron stator structure, such as the claw pole and TFMs. This paper is henceforth concerned with an MPM of the transverse flux type.

The flux path for a two-pole section of a TFM is illustrated in Fig. 1. Flux from the circumferentially magnetized magnets (1) is gathered and concentrated into the "north" pole-piece (2), traversing in the axial direction and crossing the air gap into tooth (3), across the coreback (4), and returning via the opposing tooth (5) positioned at an electrical angle of 180°, crossing the air gap once again, traversing the "south" pole piece (6) and across the magnet to complete the magnetic circuit, thus, completely enclosing the coil (7).

This 3-D flux path requires magnetic isotropy. The authors have based this study on the use of soft magnetic composites (SMCs), the properties of which are discussed in detail in [21].

Manuscript received October 28, 2011; accepted January 3, 2012. Date of publication February 10, 2012; date of current version May 18, 2012. Paper no. TEC-00536-2011.

J. G. Washington, G. J. Atkinson, N. J. Baker, A. G. Jack, and B. C. Mecrow are with the School of Electrical, Electronic and Computer Engineering, Newcastle University, Newcastle upon Tyne, NE1 7RU, U.K. (e-mail: j.g.washington@ncl.ac.uk; glynn.atkinson@ncl.ac.uk; nick.baker@ncl.ac.uk; alan.jack@ncl.ac.uk; barrie.mecrow@ncl.ac.uk).

B. B. Jensen is with the Department of Electrical Engineering, Technical University of Denmark, 2800 Kgs Lyngby, Denmark (e-mail: bbj@elektro.dtu.dk).

L.-O. Pennander, G. L. Nord, and L. Sjöberg are with the Höganäs AB, SE-263 83 Höganäs, Sweden (e-mail: Lars-olov.pennander@hoganas.com; Goran.Nord@hoganas.com; Lars.Sjoberg@hoganas.com).

Color versions of one or more of the figures in this paper are available online at http://ieeexplore.ieee.org.

Digital Object Identifier 10.1109/TEC.2012.2184115

0885-8969/$31.00 © 2012 IEEE

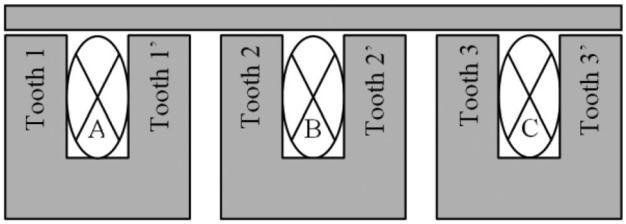

Fig. 2. Axial cross section of a three-phase separate-phase modulated pole machine.

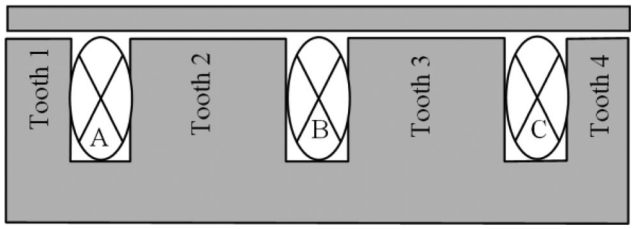

Fig. 3. Axial cross section of a three-phase combined-phase modulated pole machine.

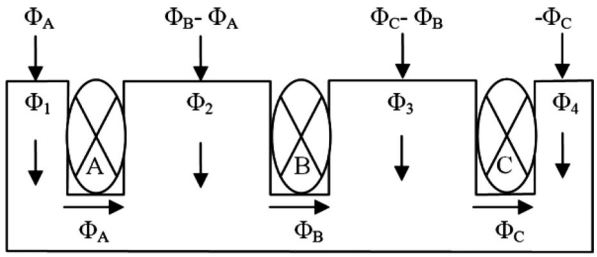

Fig. 4. Combined-phase flux paths.

This study is based on stator and rotor components built using Somaloy 3P [22].

II. Three-Phase Topologies

By the nature of their equal stator and rotor pole number, MPMs cannot produce continuous torque in a single-phase arrangement; hence they are typically used in a multiple-phase arrangement. This paper will concentrate on three-phase arrangements.

A balanced three-phase topology can be achieved by axially stacking three separate stator phases at an angular position of 0°, 120°, and 240° electrical, respectively. It is possible to use three axially separated rotors, or a single rotor extending the full axial length of the three-phase machine, as used in this study. However, in either case, the stator phases must be magnetically separated by a large distance, in relation to the air gap, to avoid mutual coupling between adjacent phases. This arrangement is illustrated in Fig. 2 and is henceforth termed a separate-phase machine.

By way of explanation, tooth 1 denotes the two teeth enclosing the coil of phase A. A north and south pole result from a circumferential angular displacement of 180° electrical between teeth 1 and 1′. Tooth 1 (phase A) is at an angular position of 0° electrical, tooth 2 (phase B) is at 120°, and tooth 3 (phase C) is at 240°. The three-phase coils are denoted by A, B, and C.

The arrangement in Fig. 2 avoids excessive mutual coupling between phases by magnetically separating the stator phases. The question arising in this study is whether there is an arrangement where these mutual flux paths can be used to an advantage?

Gieras [23] presents a three-phase transverse flux generator in which the stator phases are stacked axially with a separation between. Three rotor sections are also arranged in a similar fashion, effectively three single-phase machines of the separate-phase topology.

A similar topology has been used by Dubois *et al*. [24] in a hybrid SMC/lamination TFM stator. The stator teeth in this case form a partial claw pole. Again the three-phase arrangement comes from the stacking of three stator units, with each phase interacting with its own rotor.

Blissenbach *et al*. [25] describe a three-phase transverse flux traction motor in which a single stator structure forms three phases using circumferentially stacked laminations. The stator laminations extend the full axial length of the three-phase machine and form four teeth, partially enclosing the three-phase coils. The four teeth are bent into a position of 0°, 180°, 0°, and 180° electrically, respectively. To achieve the 120° phase shift between each of the three phases, three separate rotor units are axially stacked with a 60° offset and a magnetic gap between. The two central teeth need to carry their own and shared flux; hence, for the same magnetic flux density, the area is greater by a factor of $\sqrt{3}$. This is achieved by making the axial length of the central two teeth longer.

In this paper, the authors describe a new three-phase arrangement, termed the "combined-phase MPM" [26] in which the stator is a three-phase unit and a single rotor extends the full axial length of the machine.

Fig. 3 illustrates this new combined-phase arrangement. The internal teeth of the separate-phase topology have been combined into sets; Teeth 1′ and 2 combine to form tooth 2 of the combined-phase topology, and likewise separate-phase tooth 2′ and 3 to form combined-phase tooth 3. Hence, there are now four rather than six sets of teeth. Note however that the three coils and rotor are identical in both cases.

In order to ascertain the angular position and axial length of the four sets of teeth in the combined-phase topology, the magnetic flux in each of the four teeth is considered with the aim of producing a balanced three-phase flux linkage in each of the three coils.

Fig. 4 illustrates the tooth fluxes within the combined-phase machine. It is assumed that the amount of stray flux in this area is negligible and hence the flux directly below each coil (i.e., in the stator coreback) completely links the coil. For a balanced three-phase machine, these must be

$$\Phi_A = |\Phi| \angle 0^\circ \tag{1a}$$

$$\Phi_B = |\Phi| \angle 120^\circ \tag{1b}$$

$$\Phi_C = |\Phi| \angle 240^\circ \tag{1c}$$

where $|\Phi|$ is the magnitude of coil flux linkage (equal for all phases).

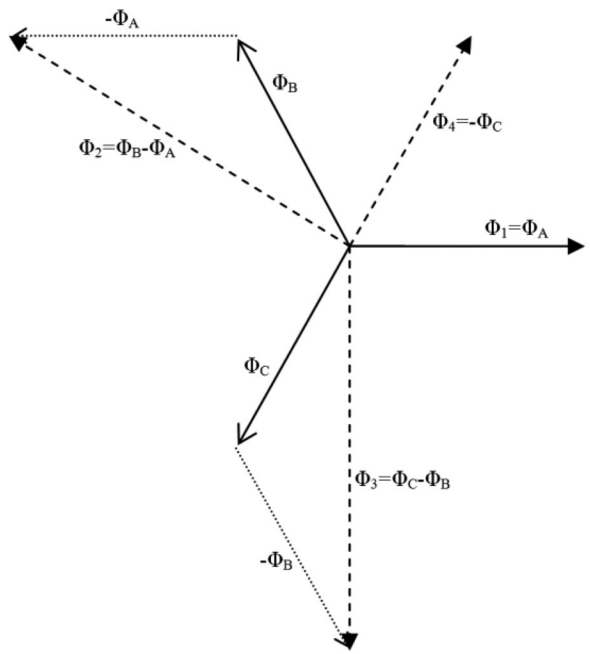

Fig. 5. Flux vector diagram showing the required tooth fluxes to achieve a balanced set of three-phase flux linkages.

If this is the case, the flux in each of the four teeth can be found by superposition

$$\Phi_1 = \Phi_A \tag{2a}$$

$$\Phi_2 = \Phi_B - \Phi_A \tag{2b}$$

$$\Phi_3 = \Phi_C - \Phi_B \tag{2c}$$

$$\Phi_4 = -\Phi_C. \tag{2d}$$

If the air-gap flux due to the rotor is assumed to be sinusoidal in space, standard vector methods can be applied to find the magnitude and angle of the flux in each tooth. In addition, the air-gap flux density is assumed to be uniform along the axis of the machine. The air-gap flux may not be sinusoidal, but the inclusion of harmonics complicates the initial analysis; instead, the fact that the air-gap flux is not a perfect sinusoid is taken into account during the finite–element (FE) modeling.

Fig. 5 shows a vector diagram of the three balanced fluxes and the resultant tooth fluxes Φ_1, Φ_2, Φ_3, and Φ_4.

Taking the resultant flux for each of the four teeth, the required tooth flux magnitude and angle is

$$\Phi_1 = |\Phi| \angle 0^\circ \tag{3a}$$

$$\Phi_2 = |\sqrt{3}\Phi| \angle 150^\circ \tag{3b}$$

$$\Phi_3 = |\sqrt{3}\Phi| \angle 270^\circ \tag{3c}$$

$$\Phi_4 = |\Phi| \angle 60^\circ. \tag{3d}$$

To maintain an equal flux density in all four teeth, the cross-sectional area of teeth 2 and 3 must be adjusted. Maintaining an identical circumferential profile (tooth angular span) means adjusting the axial length only; tooth 1 must be 1 unit long axially, teeth 2 and tooth 3 are $\sqrt{3}$ units long axially, and tooth 4 must be 1 unit long. The angular position of the tooth centers must be 0°, 150°, 270°, and 60°, respectively.

By combining the central teeth and removing the axial separation, each phase of the combined-phase machine will link more flux than its separate-phase counterpart. By applying superposition to the magnetic circuits of Figs. 2 and 3, the axial length of iron associated with each phase was found to increase by 23.1%, and it is therefore postulated that there should be an equivalent increase in phase flux. This is tested using 3-D FE methods in the following section.

III. Three-Dimensional FE Comparison

Three-dimensional FE analysis has been carried out on both the combined- and separate-phase MPMs. For this comparison both machines have identical features, as listed in the following.

1) *Dimensions:* The same overall axial length, rotor and stator outer diameter, rotor and stator inner diameter, and air-gap length.
2) *Rotor:* The same pole number, magnet type, and SMC pole pieces.
3) *Coils:* Three coils of the same inner and outer diameter, axial length, turn number, and fill factor.
4) *Materials:* NdFeB magnets with $B_R = 1.2$ T and Somaloy 3P SMC stator components and rotor pole pieces.
5) *Excitation:* An MMF of 340 A, representing a slot rms current density of 3.3 A/mm^2.

Both motors are of the outer rotor type with a rotor constructed of circumferentially magnetized NdFeB magnets sandwiched between SMC pole pieces giving a typical TFM flux concentrating arrangement.

The phases of the separate-phase machine are combined, as outlined in Section II, to form the combined-phase machine with teeth positioned at 0°, 150°, 270°, and 60° electrical. The inner two teeth are a factor of $\sqrt{3}$ axially longer than the outer two teeth.

A. FE Model

It is possible to model a single phase of an MPM and infer it's three-phase performance. This is due to the magnetic isolation given by the phase separation [8]. However, for the purposes of this comparison, it was felt that the three-phase combined-phase model must be compared to a three-phase separate-phase model. In both cases, a single pole pair of the machine is modeled with an even periodic (pole pair) boundary condition applied to the radial edges. The rotor extends the full axial length of the machine. By modeling all three phases of the separate-phase machine in the no-load condition, it was found that the peak flux linkage is 13% higher than that found in a model of a single completely isolated phase. This is due to the additional flux obtained by using a rotor that extends the full length of the stator. The additional magnet flux is provided by the magnets directly above the 2 mm gap separating the phases and also some mutual fluxes due to the proximity of phases to each other. To accurately represent this effect, the following analysis is of one pole pair of the three-phase machine.

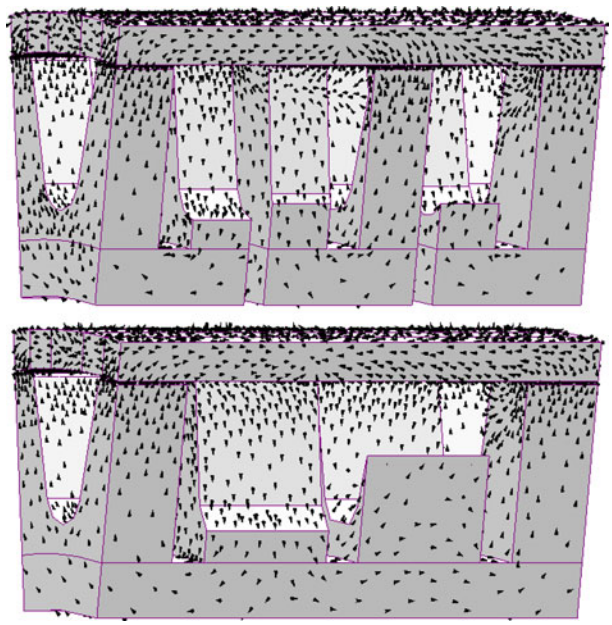

Fig. 6. Flux plots of the separate phase (top) and combined phase (bottom) with the left most phase in the aligned position.

B. No-Load Flux Linkage

The combined- and separate-phase machines were modeled in the no-load condition with the rotor aligned with tooth 1: this corresponds to the *d*-axis of phase A.

An arrow plot of the two models can be seen in Fig. 6. The isolated flux paths of the separate-phase machine are clear to see in contrast with the mutual flux paths of the combined-phase machine.

In this position, phase A of the combined-phase machine links 53.47 μWb per pole pair, compared to 48.32 μWb for the separate-phase machine; a 10.7% increase in peak flux linkage. Also taking into account the 13% increase in flux by using a rotor extending the flux axial length of the machine (including over the phase separation gaps), this is a 25.1% increase in flux linkage, slightly higher than the increase of 23.1% expected from the additional axial length of iron in the combined-phase machine.

The variation in flux linkage for the outermost phase of the separate- and combined-phase machines is shown in Fig. 7 and was obtained by performing a series of magnetostatic simulations with the rotor stepping through a full electrical cycle (two pole pitches) in increments of 5° electrical.

Fig. 8 shows the three-phase flux linkage for the combined-phase machine. The results show that all three phases are balanced with an equal 120° displacement and that the peak fluxes are within 3% of one another.

C. Back EMF

The differential of the flux waveforms yields the back EMF, as shown in Fig. 9. At 285 r/min, the rms phase back EMFs for the combined- and separate-phase machines are 28.8 and 25.8 mV per pole per turn, respectively, an increase of 11.6%

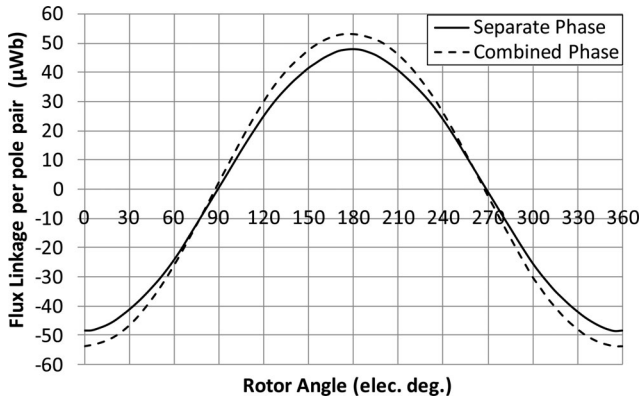

Fig. 7. Three-dimensional FE no-load flux linkage for phase A of the separate- and combined-phase machines.

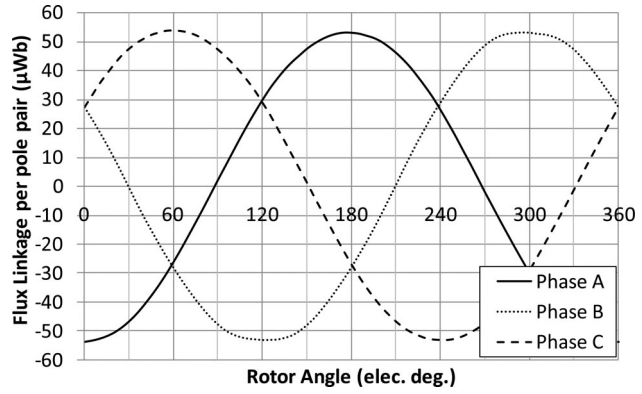

Fig. 8. No-load coil flux linkage for all three phases of the combined-phase machine.

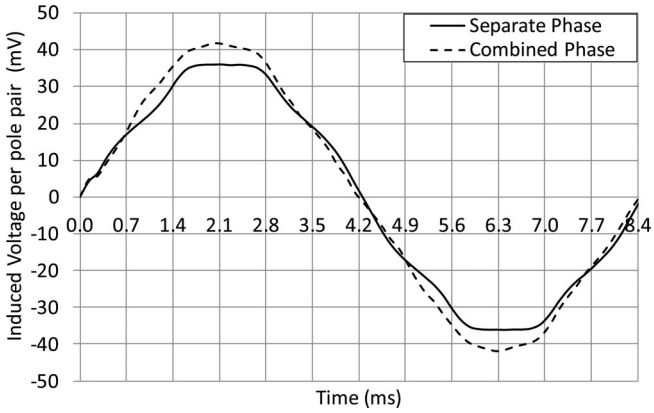

Fig. 9. Three-dimensional FE comparison of the induced back EMF in one coil of the separate- and combined-phase machines.

for the combined-phase machine. This is in line with the increase in no-load flux linkage but also reflects the fact there is some harmonic content in each of the waveforms. The fundamental components of voltage have also been compared to remove the effect of these harmonics; the combined phase shows a 13.7% increase in its fundamental component over the separate phase.

1) Static Torque: The static torque characteristics of both machines have been simulated with an MMF applied to phase 1 and returning via phases 2 and 3 connected in parallel, as

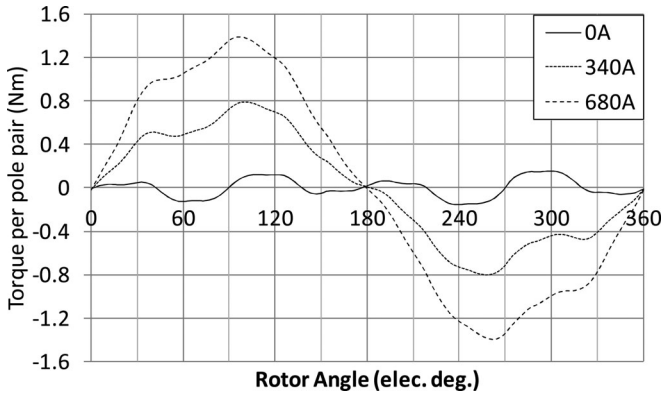

Fig. 10. Three-dimensional FE static torque characteristic for the combined-phase machine.

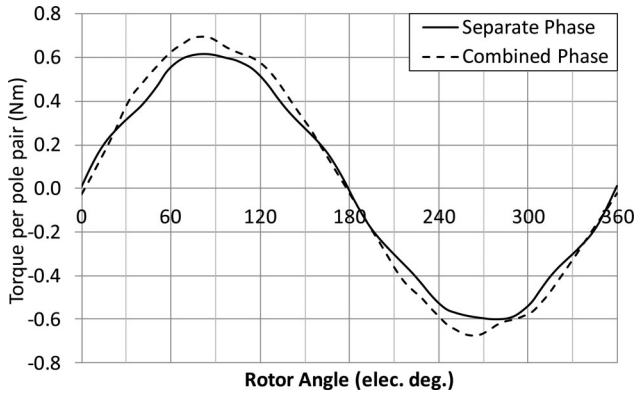

Fig. 11. Comparison of torque due to excitation for the separate- and combined-phase machines with the cogging torque removed.

in a typical experimental static torque test. The rotor steps through one-pole pair in 10° electrical steps, and the torque is obtained for MMFs ranging from 0 to 680 A [equivalent to 6.6 A/mm^2 or an overload of 2.0 per unit (p.u.)]. Fig. 10 shows the torque-position-MMF characteristics of the combined-phase machine.

The no-load cogging torque is in the order of 20% of the rated full-load torque. This level of cogging torque is significant and may be undesirable for certain applications. The authors are working on solutions to this problem, and these will form the subject of subsequent papers.

In Fig. 11, the cogging torque has been subtracted from the load torque at the rated MMF of 340 A. The rms torque for the separate- and combined-phase machines is 0.395 and 0.439 Nm per pole-pair, respectively; an 11.1% increase for the combined-phase machine.

2) Three-Dimensional FE Design Summary: A 3-D FE study of the new combined-phase MPM topology has been shown to compare favorably with the separate-phase MPM topology. Table I summarizes the results of the 3-D FE study.

IV. Experimental Validation

By way of experimental validation, a combined-phase stator and a separate-phase stator have been built; these are shown in Figs. 12 and 13, respectively. A single outer rotor has also been constructed from NdFeB magnets and SMC pole pieces; this is shown in Fig. 14. Experimental testing has been carried out with the same rotor throughout.

TABLE I
Comparison of the Separate- and Combined-Phase Modulated Pole Machine

quantity	separate phase	combined phase	percentage difference
Peak Flux Linkage	48.32 μWb	53.47 μWb	10.7
Back EMF per turn (rms)	25.8 mV	28.8 mV	11.6
Average Torque at 3.3A/mm^2	0.395 Nm	0.439 Nm	11.1
Active Mass	0.156 kg	0.162 kg	3.8
Torque Density (Average Torque) at 3.3A/mm^2	2.53 Nm/kg	2.71 Nm/kg	7.1

All quantities are per pole pair and per turn.

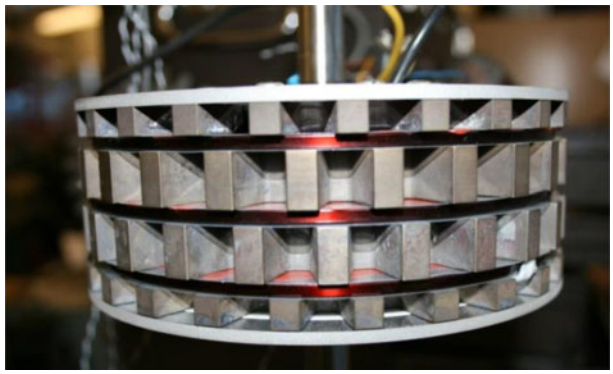

Fig. 12. Axial view of combined-phase stator.

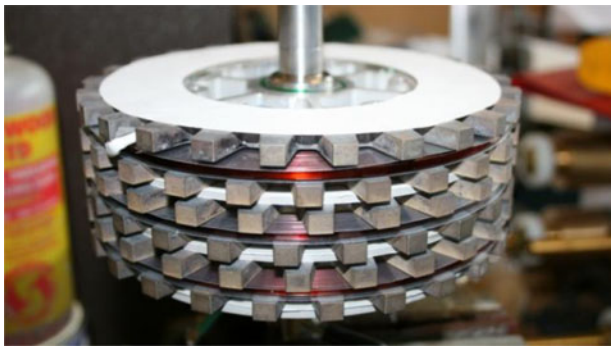

Fig. 13. Axial view of separate-phase stator.

A. Back EMF

The prototype machines were both driven on a dynamometer test rig with the armature open circuit to measure the back EMF. Both machines were star connected; the phase EMF waveforms for both prototypes were obtained and are shown in Fig. 15 at a speed of 285 r/min. Table II compares the two waveforms.

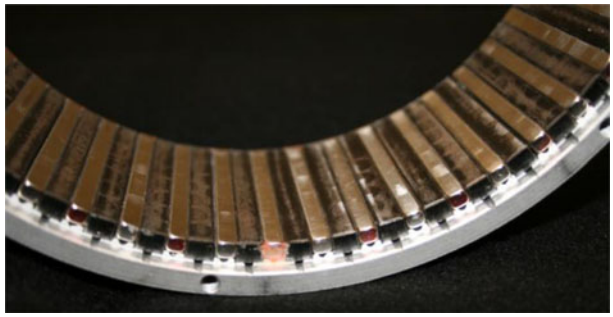

Fig. 14. Close-up view of flux concentrating rotor; the NdFeB magnets are light and the SMC pole pieces are dark.

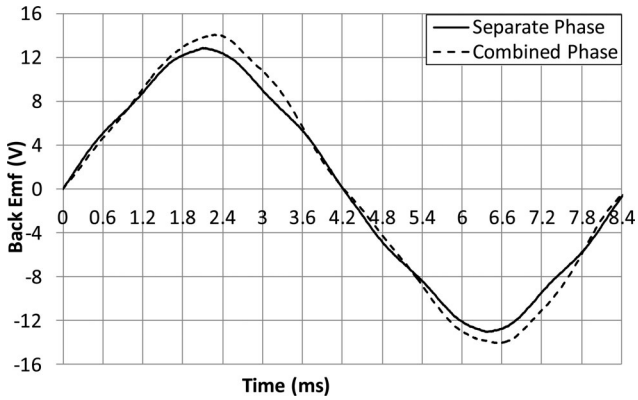

Fig. 15. Comparison of separate- and combined-phase back EMFs for one phase at 285 r/min.

TABLE II
QUANTITATIVE COMPARISON OF BACK EMF AVERAGED FOR ALL THREE PHASES OF BOTH THE MACHINES

quantity	separate phase	combined phase	percentage difference (%)
Peak Back EMF	13.26	14.38	8.47
RMS Back EMF	8.87	9.63	8.60
Fundamental Back EMF	12.52	13.82	10.34

The combined-phase machine has a 10.3% higher fundamental phase back EMF than the separate-phase machine.

B. Static Torque

Static torque was measured using an in-line torque transducer with the shaft connected to a rotary dividing head to allow for fine angular movements of the rotor, this test setup is shown in Fig. 16. The inner coil was connected in series with the outer two coils in parallel, thus, representative of a three-phase sinusoidal distribution with 1, −0.5, and −0.5 on phases 1,2, and 3, respectively.

The static torque produced over a rotation of one full electrical cycle (two pole pitches) is shown in Fig. 17. At 20 A (the thermal limit), the average per phase separate-phase torque is 7.45 Nm, compared to 8.92 Nm for the combined-phase machine.

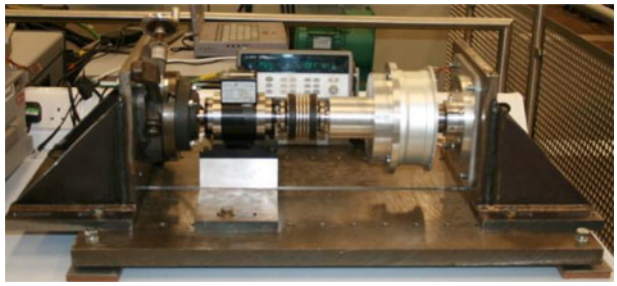

Fig. 16. Test setup showing the combined-phase machine connected through an in line torque transducer to a rotary dividing head.

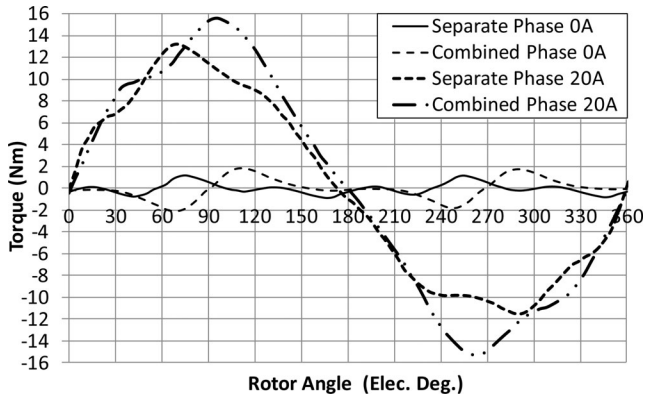

Fig. 17. Comparison of separate- and combined-phase static torque waveforms taken with maximum current in the inner phase.

The combined-phase machine shows a slightly higher level of cogging torque than the separate-phase machine; this is not a concern at this stage as this will likely be reduced by minor design modification. Further analysis of this will be considered in later publications.

The average excitation torque (i.e., the torque only due to armature current with cogging removed) produced by the combined-phase machine is 15.0% greater than the separate-phase machine. This increase is partly due to the larger back EMF and increased inductance.

C. Mass

The mass of the combined-phase machine is of course higher than the separate-phase machine as the gap between the separate phases is now taken up by iron. The active mass (SMC + copper + magnet) of the separate- and combined-phase machines is 3.89 and 4.06 kg, respectively. This is equivalent to an average torque density of 1.82 and 2.01 Nm/kg, respectively; the torque is however not that obtained under sinusoidal operating conditions and hence the torque density will be significantly higher under normal operating conditions.

D. Construction

It has been shown that a combined-phase machine will provide a higher flux linkage, higher back EMF, and higher torque within a given volume than its separate-phase counterpart. Therefore, for the same output, a combined-phase machine may be smaller.

In this analysis, the combined-phase machine has a 4.4% greater active mass than the separate-phase machine. This is due to the replacement of the phase separation by iron, but the torque per kilogram of the combined-phase machine is still 10.4% greater than that of the separate-phase machine.

In moving from a separate- to a combined-phase topology, the number of stator components is reduced from six (two halves per phase for the separate phase) to four. This reduction in component count is of a considerable benefit as the number of compactions per machine is reduced; compaction of SMC forms a significant portion of the cost of an SMC component. The reduction in component count also benefits the assembly process with fewer stages, and the removal of the phase separation results in greater mechanical integrity. It is expected that this reduction in component count as well as there been no need to manufacture phase separators will lead to the overall cost of the combined-phase machine being reduced in comparison to the separate phase.

V. Conclusion

MPMs, a term describing both transverse flux and claw pole machines, are well known for their high torque density. This comes at the cost of a higher electrical frequency, a characteristic making MPMs particularly suited to low-speed high-torque applications, such as direct drive traction machines.

The nature of their design means that they cannot provide continuous torque in a single-phase arrangement; hence, a multiphase arrangement is required. This paper has investigated three-phase MPMs.

The most obvious arrangement is to axially stack the three phases, with a small separation between to avoid flux leakage between phases. If a single rotor is used spanning the axial length of the three phases, the magnet above the phase separation is wasted.

The authors have described an alternative three-phase arrangement, which takes advantage of mutual flux paths between phases and removes the phase separations. This combined-phase MPM has been analyzed along with its separate-phase counterpart, using an identical space envelope, rotor, coils, and material properties.

Simulations show an improved electromagnetic performance for the combined-phase machine, validated by prototype testing. Two machines were built, sharing the same rotor. Experimentation confirmed the improved performance of the combined-phase machine, with a 10.3% increase in fundamental back EMF (corresponding to a 8.6% increase in rms back EMF), a 15.0% increase in the average excitation torque, and a 10.4% higher torque density when compared to the separate-phase machine. These results are shown in Table III.

In addition to the improved electromagnetic performance, the combined-phase machine offers a reduction in stator SMC components from six to four. This is clearly of great benefit in terms of commercial production, with fewer components and greater mechanical integrity of the stator.

Of continuing interest to the authors is work in reducing harmonic content and cogging torque of the combined-phase machine.

TABLE III
Comparison of the Separate- and Combined-Phase Modulated Pole Machine Electromagnetic Performance

quantity	separate phase	combined phase	percentage differene (%)
Per phase back EMF @ 285rpm (rms)	8.87 V	9.63 V	8.6
Average Thermal limit torque (cogging neglected)	7.08 Nm	8.14 Nm	15.0
Active mass.	3.89 kg	4.06 kg	4.4
Torque Density (Average Torque)	1.82 Nm/kg	2.01 Nm/kg	10.4

References

[1] W. M. Mordey, "Electric generator," United States Patent No. 437501, Sep. 30, 1890.

[2] C. P. Maddison, B. C. Mecrow, and A. G. Jack, "Claw pole geometries for high performance transverse flux machines," in *Proc. Int. Conf. Electr. Mach.*, Istanbul, Turkey, 1998, pp. 340–345.

[3] G. Jack, B. C. Mecrow, C. P. Maddison, and N. A. Wahab, "Claw pole armature permanent magnet machines exploiting soft iron powder metallurgy," in *Conf. Rec. IEEE Int. Electr. Mach. Drives*, 1997, pp. MA1/5.1–MA1/5.3.

[4] B C. Mecrow, A. G. Jack, and C. P. Maddison, "Permanent magnet machines for high torque, low speed applications," in *Proc. 12th Int. Conf. Electr. Mach.*, Vigo, Spain, 1996, pp. 461–466.

[5] H. Weh and H. May, "Achievable force densities for permanent magnet excited machines in new configurations," in *Proc. Int. Conf. Electr. Mach.*, 1986, pp. 1107–1111.

[6] W. M. Arshad, T. Backstrom, and C. Sadarangani, "Analytical design and analysis procedure for a transverse flux machine," in *Proc. Electr. Mach. Drives Conf.*, 2001, pp. 115–121.

[7] Y. G. Guo, J. G. Zhu, P. A. Watterson, and W. Wu, "Development of a PM transverse flux motor with soft magnetic composite core," *IEEE Trans. Energy Convers.*, vol. 21, no. 2, pp. 426–434, Jun. 2006.

[8] D. H. Kang and H. Weh, "Design of an integrated propulsion, guidance, and levitation system by magnetically excited transverse flux linear motor (TFM-LM)," *IEEE Trans. Energy Convers.*, vol. 19, no. 3, pp. 477–484, Sep. 2004.

[9] H. M. Hasanien, A. S. Abd-Rabou, and S. M. Sakr, "Design optimization of transverse flux linear motor for weight reduction and performance improvement using response surface methodology and genetic algorithms," *IEEE Trans. Energy Convers.*, vol. 25, no. 3, pp. 598–605, Sep. 2010.

[10] H. M. Hasanien, "Particle swarm design optimization of transverse flux linear motor for weight reduction and improvement of thrust force," *IEEE Trans. Ind. Electron.*, vol. 58, no. 9, pp. 4048–4056, Sep. 2011.

[11] A. S. Abd-Rabou, H. M. Hasanien, and S. M. Sakr, "Design development of permanent magnet excitation transverse flux linear motor with inner mover type," *IET Proc. Electr. Power Appl.*, vol. 4, no. 7, pp. 559–568, Aug. 2010.

[12] S. Baserrah and B. Orlik, "Comparison study of permanent magnet transverse flux motors (PMTFMs) for in-wheel applications," in *Proc. Int. Conf. Power Electron. Drive Syst.*, 2009, pp. 96–101.

[13] Heetae, J. Gunhee, C. Junghwan, C. Shiuk, and K. Dohyun, "Reduction of the torque ripple and magnetic force of a rotatory two-phase transverse flux machine using herringbone teeth," *IEEE Trans. Magn.*, vol. 44, no. 11, pp. 4066–4069, Nov. 2008.

[14] J. Mitcham, "Transverse flux motors for electric propulsion of ships," presented at the IEE Colloq. New Topologies Permanent Magnet Mach., London, U.K., 1997.

[15] E. Schmidt, "3-D finite element analysis of the cogging torque of a transverse flux machine," *IEEE Trans. Magn.*, vol. 41, no. 5, pp. 1836–1839, May 2005.

[16] E. Schmidt, "Finite element analysis of a novel design of a three phase transverse flux machine with an external rotor," *IEEE Trans. Magn.*, vol. 47, no. 5, pp. 982–985, May 2011.

[17] M. Dubois, "Optimized permanent magnet generator topologies for direct drive wind turbines," Ph.D. dissertation, Delft Univ. Technol., Delft, The Netherlands, 2004.

[18] H. Polinder, B. C. Mecrow, A. G. Jack, P. G. Dickinson, and M. A. Mueller, "Conventional and TFPM linear generators for direct-drive wave energy conversion," *IEEE Trans. Energy Convers.*, vol. 20, no. 2, pp. 260–267, Jun. 2005.
[19] J. Vining, T. A. Lipo, and G. Venkataramanan, "Design and optimization of a novel hybrid transverse/longitudinal flux, wound-field linear machine for ocean wave energy conversion," in *Proc. IEEE Energy Convers. Congr. Expo.*, 20–24 Sep. 2009, pp. 3726–3733.
[20] M. R. Harris, G. H. Pajooman, and S. M. Abu Sharkh, "The problem of power factor in VRPM (transverse-flux) machines," in *Proc. 8th Int. Conf. Electr. Mach. Drives*, 1997, pp. 386–390, Conf. Publ. No. 444.
[21] A. G. Jack and L-O. Pennander, "Soft magnetic iron powder materials A.C. properties and their application in electrical machines," presented at the EURO PM, Valencia, Spain, 2003.
[22] "Somaloy technology for electric motors," (Mar. 2011). [Online]. Available: http://www.hoganas.com
[23] J. F. Gieras, "Performance characteristics of a permanent magnet transverse flux generator," in *Proc. IEEE Int. Conf. Electr. Mach. Drives*, San Antonio, Texas, May 2005, pp. 1293–1299.
[24] M. R. Dubois, N. Dehlinger, H. Polinder, and D. Massicotte, "Clawpole transverse-flux machine with hybrid stator," presented at the Int. Conf. Electr. Mach., Chania, Greece, 2006.
[25] R. Blissenbach, G. Henneberger, U Schafer, and W Hackman, "Development of a transverse flux traction motor in a direct drive system," in *Proc. Int. Conf. Electr. Mach.*, Espoo, Finland, 2000, pp. 1457–1460.
[26] G. J. Atkinson, A. G. Jack, and B. C. Mecrow, "Multi-phase stator device," Patent W0/2011/033106, Published Mar. 24 2011.

Jamie G. Washington received the B.Eng. degree in electrical and electronic engineering from Newcastle University, Newcastle Upon Tyne, U.K., in 2008, where he is currently working toward the EngD degree sponsored by Hoganas AB. His EngD thesis focuses on high-torque low-speed machines constructed using soft magnetic composites.

Glynn J. Atkinson received the M.Eng. degree in electrical and electronic engineering from Newcastle University, Newcastle Upon Tyne, U.K., in 2001. His EngD degree focused on fault-tolerant machines for aerospace applications, focusing on high-power, high-speed permanent magnet machines.

He was a Research Associate in the power electronics, machines, and drives group at Newcastle University, Newcastle upon Tyne, where he was engaged in research on 3-D machine topologies using soft magnetic composites, and is currently a Lecturer within the group leading research into permanent magnet machine topologies for use in traction applications.

Nick J. Baker received the M.Eng. degree in mechanical engineering from Birmingham University, Birmingham, U.K., in 1999, and the Ph.D. degree in electrical machine design for marine renewable energy devices from Durham University, Durham, U.K., in 2003.

He has held research posts in machine design at Durham University. He is currently with Newcastle University, Newcastle upon Tyne, U.K., in addition to an academic post within Lancaster University's Renewable Energy Group (2005–2008). From 2008 to 2010, he was a Senior Consultant for energy consultancy TNEI, Newcastle, U.K.

Alan G. Jack received the Ph.D. degree from Southampton University, Southampton, U.K., in 1975. His Ph.D. thesis focused on numerical analysis of electromagnetic fields in turbogenerators.

He is currently the Emeritus Professor in Electrical Engineering, formally the Chair of Electrical Engineering, and the Head of the Department and leader of the Newcastle Electric Drives and Machines Group, Newcastle University, Newcastle upon Tyne, U.K. He has been with the University for more than 20 years, joining them from NEI Parsons, where he was for 13 years with roles from craft apprentice to principal design engineer. He is the author of more than 80 papers in the area of electrical machines and drives.

Barrie C. Mecrow received the Ph.D. degree from Newcastle University, Newcastle Upon Tyne, U.K., in 1987, his thesis focused on 3-D eddy current computation applied to turbogenerators.

He was a turbogenerator Design Engineer with NEI Parsons, Newcastle Upon Tyne, U.K., until 1987. In 1987, he became a Lecturer at the University of Newcastle, Newcastle Upon Tyne, where he is currently a Professor of Electrical Power Engineering. He is involved in a range of research projects, including fault-tolerant drives, high-performance permanent magnet machines, and novel switched reluctance drives.

Bogi B. Jensen received the Ph.D. degree from Newcastle University, Newcastle Upon Tyne, U.K. His Ph.D. thesis focused on toroidally wound induction machines.

From 1994 to 2002, he was in the marine sector with roles from Engineering Cadet to Senior Field Engineer. In 2002, he joined academia as a Lecturer at the Centre of Maritime Studies and Engineering, Faroe Islands. He moved to the United Kingdom in 2004 and became a Research Associate in 2007 and a Lecturer in 2008, both at Newcastle University. He is currently an Associate Professor of Electrical Machines at the Centre for Electric Technology, Department of Electrical Engineering, Technical University of Denmark (DTU), Kongens Lyngby, Denmark. His major research interests include electrical machine design, analysis, and development.

Lars-Olov Pennander received the M.Sc. and Ph.D. degrees from the Department of Materials Engineering and Production Technology, LTH/Lund University, Lund, Sweden, in 1985 and 1998, respectively. His M.Sc. thesis focused engineering materials, machine design, and production technology, and the Ph.D. thesis focused on giant-magnetostrictive actuation of metal–matrix composite material production systems.

In 1981, he was a technical officer in the Swedish Air Force. In 2001, he became a Development Engineer with the world leading supplier of metal powders, Höganäs AB, Höganäs, Sweden, where he was engaged in research on magnetic applications for soft magnetic powder composites in electrical machines and is currently involved in research on the analysis and development of powder-core inductor applications for power electronics.

Göran L. Nord received the M.Eng. degree in engineering physics from Lund Institute of Technology, Lund, Sweden, in 1987.

He was an Electromagnetic Equipment Designer for the steel industry with ABB until 1992, where he was also engaged in research with trains in the field of mechanical drive system and vehicle dynamics until 1996. From 1996 until 2001, he was an electric machine designer with Emotron, where he was engaged in research on switched reluctance motors and high-speed electrical drive systems. Since 2001, he has been an Application Specialist and permanent magnet machine designer with Höganäs AB, Höganäs, Sweden.

Lars Sjöberg received the M.Sc. degree in electrical engineering, in 1992, and the Tech. Lic. degree from the Department of Industrial Electrical Engineering and Automation, LTH/Lund University, Lund, Sweden, in 1996. His Tech. Lic. thesis focused on torque control and design of switched reluctance motors based on soft magnetic composite materials.

In 1996, he became an electric machine designer at Emotron AB, where he was engaged in research on switched reluctance motors. In 2002, he was with Danaher Corporation, where he was involved in research on electric machine design, mainly induction and permanent magnet machines. From 2003 to 2008, he was a manager for the Electro and Power Supply Group at the Swedish Railway Training Centre. Since 2009, he has been an application specialist with Höganäs AB, Höganäs, Sweden, where he is currently a Manager for the electric machine design team engaged in the design of novel torque-dense motors based on soft magnetic composite material.